3D flyable curves for an autonomous aircraft

Cite as: AIP Conference Proceedings **1493**, 132 (2012); https://doi.org/10.1063/1.4765481
Published Online: 06 November 2012

Yasmina Bestaoui

3D Flyable Curves for an Autonomous Aircraft

Yasmina Bestaoui

Laboratoire IBISC, Universite d'Evry, France

Abstract. The process of conducting a mission for an autonomous aircraft includes determining the set of waypoints (flight planning) and the path for the aircraft to fly (path planning) .
The autonomous aircraft is an under-actuated system, having less control inputs than degrees of freedom and has two non-holonomic (non integrable) kinematic constraints. Consequently, the set of feasible trajectories will be restricted and the problem of trajectory generation becomes more complicated than a simple interpolation. Care must be taken in the selection of the basic primitives to respect the kinematic and dynamic limitations.
The topic of this paper is trajectory generation using parametric curves. The problem can be formulated as follows: to lead the autonomous aircraft from an initial configuration q_i to a final configuration q_f in the absence of obstacles, find a trajectory q(t) for $0 \leq t \leq T$. The trajectory can be broken down into a geometric path q(s), s being the curvilinear abscissa and s=s(t) a temporal function. In 2D the curves fall into two categories:

- Curves whose coordinates have a closed form expressions, for example B-splines, quintic polynomials or polar splines
- Curves whose curvature is a function of their arc length for example clothoids, cubic spirals, quintic or intrinsic splines

Some 3D solutions will be presented in this paper and their effectiveness discussed towards the problem in hand.

Keywords: Autonomous Aircraft, flight plan, path planning
PACS: 02.70, 07.05, 02.30

INTRODUCTION

Autonomous aircrafts are replacing the human-piloted aircrafts in many applications. The replacement of the human operator in such systems necessitates the development of autonomous systems techniques. Trajectory planning is an important issue in the development of autonomous aircrafts.
The route is usually defined by a set of waypoints joined by straight line segments, which connect the start and goal way points and hence may not be flyable because the autonomous aircraft cannot turn instantaneously through each way point. A flyable path is designed by interpolating the positions, directions and curvature at the waypoints and end-points [9].
This paper deals with the evolution of the flight path and design of a feasible flight automatically to fly from one way point to another, six parameters being taken into account: their position, their orientation given by heading and flight path angles and velocities. Feasible trajectories should respect the limitation of vehicle performances under specific constraint conditions. Examples of such constraints include minimum turning radius and minimum and maximum speed of the autonomous aircraft, as well as dynamic limitations on thrust and angle of attack. Developing methods for trajectory planning must be sufficiently fast.
2D path planning concerns the motion of an aircraft to a plane. If the plane is horizontal, this is equivalent to flying at a constant altitude. The plane can also be inclined at an angle to facilitate a change in altitude if required. Path planning in 2D space is abundant in the literature, due to the fact that path planning is also studied in ground robotics [13, 15, 17, 18, 23] . However, when dealing with aerial vehicles, altitude has to be added to the planar movement for maneuvers in space. There are only a few references to work done on path planning in 3D mostly based on a generalization of Dubbins curves [1, 3, 22, 24], while a few consider the Frenet-Serret frame [2, 5, 4, 20].
Autonomous aircrafts belong in the category of finite dimensional mechanical systems known as nonholonomic systems. Non holonomy means that the velocity constraints are not integrable, indicating that some configurations in the velocity space, i.e. directions of movements are not possible.
In contrast to trajectory generation for holonomic systems there is no one-to-one correspondence between available paths and feasible trajectories. Only the motions that satisfy the nonholonomic constraints are allowed. By considering the realistic assumption that the aircraft is completely controllable at least one feasible path exists for every pair of way points.
In 3D, flyable paths must take into account both curvature and torsion in their design. Curvature defines the turn radius of the path in 2D, which is defined as a rotation about an axis normal to the manoeuvre. Torsion is defined as a rotation about an axis that coincides with the path tangent vector. In terms of body axes, curvature is equivalent to a yaw rate turn and torsion is equivalent to

9th International Conference on Mathematical Problems in Engineering, Aerospace and Sciences
AIP Conf. Proc. 1493, 132-139 (2012); doi: 10.1063/1.4765481

roll rate turn.
By satisfying the curvature and torsion constraints, the motion of the aircraft stays within its maximum-curvature (acceleration) bounds. The curvature is proportional to the lateral acceleration, thus the curvature at any point on the path must be less than the maximum curvature constraint of the autonomous aircraft.
The issues of continuity of the curvature and its derivative have led to 2D parametric curves such as polar polynomial, cubic spiral [4, 15] sums of sine and cosine, Pythagorean Hodograph curve, parameter splines of higher order [10, 11], uniform quartic B- splines, η^3 splines [19] .
The contribution of this paper is the generation of a flyable curve via the Double Pythagorean Hodograph (DPH) curves, taking into account the limitations of the curvature and torsion.
This paper is organized as follows: Problem formulation is proposed in Section 2. Trim trajectories are presented in Section 3 while the 2D and 3D maneuver approaches using Polynomial curves and Double Pythagorean Hodographs with Bernstein-Bezier polynomials, are presented with some simulation results in Section 4, finally some conclusions are given in section 5.

PROBLEM FORMULATION

For the purpose of flight path generation, it is usually sufficient to treat only the translational motion.

Kinematic and Dynamic Models

The translational equations of an aerospace vehicle through the atmosphere are directly derived from Newton's law. The variables x, y, z are the autonomous aircraft inertial coordinates. The flight path coordinate system relates the velocity vector of the vehicle with respect to Earth geographic system. The heading angle χ is measured from North to the projection of V (the autonomous aircraft velocity relative to the wind) in the local tangent plane and the flight path angle γ takes vertically up to V. The x, y directions are chosen such that the xy plane is horizontal, the x-direction is aligned with the principal axis of symmetry and the z-direction is ascending vertically.
The translational kinematics of an aerial vehicle can be expressed by the following equations:

$$\begin{aligned} \dot{x} &= V\cos\chi\cos\gamma \\ \dot{y} &= V\sin\chi\cos\gamma \\ \dot{z} &= V\sin\gamma \end{aligned} \tag{1}$$

Where V is the autonomous aircraft velocity relative to the wind, $\dot{x}(t)=\frac{dx}{dt}, \dot{y}(t)=\frac{dy}{dt}$ and $\dot{z}(t)=\frac{dz}{dt}$
The dynamic model can be written as:

$$\dot{V} = -gsin\gamma + \frac{1}{m}(Tcos\alpha - D) \tag{2}$$

$$\dot{\chi} = \frac{L+Tsin\alpha}{mVcos\gamma}(sin\sigma) \tag{3}$$

$$\dot{\gamma} = \frac{Tsin\alpha + L}{mV}cos\sigma - \frac{g}{V}cos\gamma \tag{4}$$

The direction of the velocity V is denoted by the heading angle χ, flight path angle γ and bank angle σ. The bank angle is the angle between the aircraft lift and weight force vectors. The aircraft velocity V is assumed to be equal to the airspeed. The parameters D and L are respectively the drag and lift forces, m is the aircraft mass and g is the acceleration due to gravity. The lift and drag can be expressed as a function of a non dimensional drag coefficient C_L, C_D in the form

$$\begin{aligned} L &= \tfrac{1}{2}\rho V^2 S C_L \\ D &= \tfrac{1}{2}\rho V^2 S C_D \end{aligned} \tag{5}$$

where S is the aerodynamic reference area and ρ is the averaging density of the air, considered to be constant. The following relationship is classically used :

$$C_D = C_{D_0} + KC_L^2 \tag{6}$$

where C_{D_0} is the profile drag coefficient and KC_L is the induced drag. Replacing the lift coefficient with the load factor, the drag D can be computed as:

$$D = \frac{1}{2}\rho V S C_{D_0} + 2K\frac{L^2}{\rho V^2 S} \tag{7}$$

The path planning generates a feasible flight path for an aerial vehicle to reach the target. Geometrically, they are the solution of this system.

Frenet-Serret Frame

The shape of a space curve can be completely captured by its curvature and torsion.The tangent T, normal N and binormal B of the curve C, in the Frenet Serret frame, are defined as:

$$T = \frac{C'}{\|C'\|} \quad N = \frac{C'\times C''}{\|C'\times C''\|} \quad B = T\times N \tag{8}$$

This tangent is constrained to have unity norm ($'$ represents derivation versus the curvilinear abscissa s). κ is called the curvature of the motion :

$$\kappa = \frac{C'\times C''}{\|C'\|^3} \tag{9}$$

and the torsion of the motion is

$$\Gamma = \frac{(C' \times C'').C'''}{\|C' \times C''\|^2} \tag{10}$$

If a non vanishing curvature and a torsion are given as smooth functions of s, theoretically both equations can be integrated to find the numerical values of the corresponding space curve (up to a rigid motion). The shape of a 3D curve can be completely captured by its curvature and torsion functions. Hence, they are considered to be a set of intrinsic and complete shape features of the curve C and expressed by the differential system [16]. Thus, the differential equation describing the evolution of the Frenet-Serret formula for parameterized curves in $\Re^3$ can be written as:

$$\frac{d\Phi}{ds} = \begin{pmatrix} \dot{T} \\ \dot{N} \\ \dot{B} \end{pmatrix} = V(t) \begin{pmatrix} 0 & \kappa & 0 \\ -\kappa & 0 & \Gamma \\ 0 & -\Gamma & 0 \end{pmatrix} \begin{pmatrix} T \\ N \\ B \end{pmatrix} \tag{11}$$

where

$$Sk \begin{pmatrix} \Gamma \\ 0 \\ \kappa \end{pmatrix} = \begin{pmatrix} 0 & \kappa & 0 \\ -\kappa & 0 & \Gamma \\ 0 & -\Gamma & 0 \end{pmatrix} \tag{12}$$

$Sk(.)$ is the skew matrix associated to the vector $(.)$
The length of the Darboux vector, also called total curvature, includes both of the above features:

$$\Theta = \Gamma T + \kappa B \tag{13}$$

Θ indicates how the entire frame rotates, making it the measure of the structural variation in C. The entire frame rotate about Θ at the angular rate of $\|\Theta\|$.
The Frenet-Serret frame equations are pathological for example when the curve is perfectly straight or when the curvature vanishes momentarily. The case $\kappa = \tau = 0$ corresponds to changing signs at special curve points.

Non holonomic Problem

The curvilinear abscissa s being considered instead of the time, the curve C represents the motion of this vehicle in R^3,where

$$V = \frac{ds}{dt} \tag{14}$$

In 3D space, the following flight path is characterized by:

$$\begin{aligned} dx &= \sin\chi \cos\gamma ds \\ dy &= \cos\chi \cos\gamma ds \\ dz &= \sin\gamma ds \end{aligned} \tag{15}$$

Two non-holonomic constraints can thus be deduced:

$$\begin{aligned} dx\cos\chi - dy\sin\chi = 0 \\ \{dx\sin\chi + dy\cos\chi\}\sin\gamma - dz\cos\gamma = 0 \end{aligned} \tag{16}$$

These conditions that must be verified at all points by the tangent vector on the configuration space path, characterize the motion of geometric path admissibility induced by the kinematic constraint that actually affects generalized velocities.
For non holonomic vehicles such as mobile or autonomous aircrafts, dynamic model and actuators constraints that directly affect path are used to reject infeasible paths. The term feasible means that the path will be continuously flyable and safe. The flyable path should be smooth, i.e without twists and cusps. The smoothness of the path is determined by amount of bending of the path, measured by curvature and torsion of the path [2, 1].
Using the Frenet-Serret formulation (9),curvature κ can be deduced:

$$\kappa = (\gamma'^2 + \chi'^2 cos^2\gamma)^{-1/2} \tag{17}$$

as well as the torsion Γ as:

$$\begin{aligned} \Gamma = \frac{\chi'\gamma''\cos\gamma + 2\chi'\gamma'^2\sin\gamma - \gamma'\chi''\cos\gamma}{\gamma'^2 + \chi'^2\cos^2\gamma} + \\ + \frac{-\gamma'\chi'^2\cos\chi\cos\gamma\sin^2\gamma\sin\chi + \chi'^3\sin\gamma\cos^2\gamma}{\gamma'^2 + \chi'^2\cos^2\gamma} \end{aligned} \tag{18}$$

All maneuvers can be defined by reference to a set of axes. These can be fixed in inertial space or defined relative to a set of axes that are attached to the path defined by a curve known as the Frenet-Serret frame framework, or a newly defined known as the Euler frame.
It is essential to have an on-board processor to design and execute paths and trajectories.
To lead the autonomous aircraft from the i^{th} configuration $q(t_i) = q_i$ to a $(i+1)^{th}$ configuration $q(t_f) = q_f$ in the absence of obstacles, a trajectory $q(t)$ for $t \in [0, t_f]$ has to be planned [6]. The output is a parametric curve. At a given speed V, the lateral acceleration a is proportional to the curvature κ, such that $|a| = V^2\kappa$
The purpose of the following sections is to propose a 3D flight path to the aerial vehicle joining two successive waypoints configurations, for $i = 1, .., N$.
The inputs of this path planning algorithm are :

- the i^{th} configuration : $q_i = (x_i, y_i, z_i, \gamma_i, \chi_i, V_i)$
- the $(i+1)^{th}$ configuration : $q_f = (x_f, y_f, z_f, \gamma_f, \chi_f, V_f)$.

The limitations on the curvature and the torsion

$$|\kappa| \leq \kappa_{max} \qquad |\Gamma| \leq \Gamma_{max} \tag{19}$$

can be computed using the dynamic limitations on the thrust, bank angle and angle of attack, as the curvature et

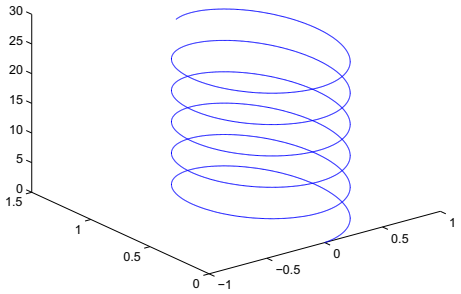

FIGURE 1. Trim Path

torsion can be written as a function of thrust, bank angle and angle of attack:

$$\kappa = \sqrt{(\frac{T sin\alpha + L}{mV^2} cos\sigma - \frac{g}{V^2} cos\gamma)^2 + (\frac{L + T sin\alpha}{mV^2} (sin\sigma))^2} \tag{20}$$

TRIM FLIGHT PATHS

In this case, the flight path angle γ is constant while the angle χ is linearly varying versus s.

$$\chi(s) = \chi_0 + s\chi_1 \tag{21}$$

The parameters γ_0, χ_0, χ_1 being constants, the following relations can be proposed :

$$x(s) = x_i + \frac{\cos\gamma_0}{\chi_1} (\cos(\chi_0 + \chi_1 s) - \cos\chi_0) \tag{22}$$

$$y(s) = y_i - \frac{\cos\gamma_0}{\chi_1} (\sin(\chi_0 + \chi_1 s) - \sin\chi_0) \tag{23}$$

$$z(s) = s\sin(\gamma_0) + z_i \tag{24}$$

It is a well-known fact that trim trajectories are represented in general by helices, with particular cases: straight motion or circle arcs, (see figure 1) (The units are in 10Km).
This particular case occurs when $\gamma_i = \gamma_f$ and the following relationships are verified

$$\chi_1 = \sin(\gamma_i) \frac{\chi_f - \chi_i}{z_f - z_i} \tag{25}$$

with the constraint between the initial and final positions:

$$[\chi_1(x_f - x_i) + \cos\gamma_i \sin\chi_i]^2 + [\chi_1(y_f - y_i) - \cos\gamma_i \cos\chi_i]^2 = \cos^2\gamma_i \tag{26}$$

L the length of the path being given by

$$L = \frac{\chi_f - \chi_i}{\chi_1} \tag{27}$$

For this kind of curves, curvature and torsion are constant

$$\begin{aligned} \kappa(s) &= \chi_1 \cos(\gamma_0) \\ \Gamma(s) &= \chi_1 \sin(\gamma_0) \end{aligned} \tag{28}$$

The role of the trajectory generator is to generate a feasible time trajectory for the aerial vehicle. Only trim flight paths respecting the curvature and torsion constraints are acceptable.

PARAMETRIC CURVES FOR MANEUVERS

Path planning focuses on finding a path through free space from two successive way-points. The focus in this section in on turning a sequence of configurations into a smooth curve that is then passed to the control system of the vehicle.
An exact fit would involve interpolation, an approximate fit might involve least-square approximation or the smoothing spline. If a function is to be approximated over a large interval, the degree n of the approximating polynomial may have to be chosen unacceptably large. The alternative is to subdivide the interval $[a,b]$ of approximation into sufficiently small intervals $[\xi_j, \xi_{j+1}]$ with $a = \xi_1 < ... < \xi_{N+1} = b$ so that on each sub-interval, a polynomial P_j of relatively low degree can provide a good approximation to f. This can be done in such a way that the polynomial pieces blend smoothly, i.e., so that the resulting composite function has several continuous derivatives. Any such smooth piecewise polynomial function is called a spline [7, 8, 19].
Transition curves are used for blending in the plane that is to round corners or for smooth transition between straight lines and circular arcs, two circular arcs or two straight lines. The resulting curves should have position and curvature continuity as well as continuity of the unit tangent vector. Such continuity is usually referred to in the Computer Aided Geometric Design as G^2 Continuity. Higher order of continuity G^k will ensure smoother transition curve with direct physical meaning on moving the autonomous aircraft along its path.
In 2D the curves fall into two categories

- Curves whose coordinates have a closed form expressions for example B-splines, quintic polynomials or polar splines
- Curves whose curvature is a function of their arc length for example clothoids, cubic spirals, quintic G^2 splines or intrinsic splines

Non trim Trajectories at Constant altitude

The initial $P_i = (x_i, y_i, \chi_i)^T$ and final configurations $P_f = (x_f, y_f, \chi_f)^T$ are said symmetrical if $\zeta = \frac{\chi_i + \chi_f}{2}$ where $\varsigma = \arctan \frac{y_f - y_i}{x_f - x_i}$ the orientation of P_f versus P_i. Let's define the Euclidean distance $d = \sqrt{(x_f - x_i)^2 + (y_f - y_i)^2}$ and the deflection $\zeta = \chi_f - \chi_i$. A path is represented by the pair (ℓ, κ) where ℓ is a positive length and $\kappa : \left[-\frac{\ell}{2}, \frac{\ell}{2}\right]$. Let's suppose that $x(0) = y(0) = \chi(0) = 0$. Knowing the path curvature $\kappa(s)$ and initial conditions allow the construction of the path:

$$\begin{aligned} \chi(s) &= \int_0^s \kappa(u)du \\ x(s) &= \int_0^s \sin(\chi(u))du \\ y(s) &= \int_0^s \cos(\chi(u))du \\ 0 \leq s \leq \ell & \end{aligned} \tag{29}$$

Clothoids. The curvature of a clothoid curve is proportional to the length of the path as a curve element $\kappa(s) = \sigma_c s$, where σ_c is a real constant called the sharpness of the Clothoid [13, 15].
An elementary path is considered as a concatenation of two equal piecewise clothoids.

$$\begin{aligned} \kappa(s) &= \sigma_c s & \forall s \in \left[0, \tfrac{\ell}{2}\right] \\ \kappa(s) &= \sigma_c(\ell - s) & \forall s \in \left[\tfrac{\ell}{2}, \ell\right] \end{aligned} \tag{30}$$

Furthermore, two configurations in the plane can be obtained with two different elementary paths to form a bi-elementary path. In particular to link two successive way-points $P_i = (x_i, y_i, \chi_i)^T, P_f = (x_f, y_f, \chi_f)^T$, it is necessary to calculate the split configurations $P_s = (x_s, y_s, \chi_s)^T$ which is a symmetric configurations with respect to the start and end configurations. For symmetrical configurations, the following relations are verified

$$\begin{aligned} \kappa\left(\tfrac{\ell}{2}\right) &= -\kappa\left(-\tfrac{\ell}{2}\right) \\ \chi\left(\tfrac{\ell}{2}\right) &= \chi\left(-\tfrac{\ell}{2}\right) = \tfrac{\zeta}{2} \\ D(\zeta) &= 2\int_0^{0.5} \sin(2\zeta u^2)du \end{aligned} \tag{31}$$

$\Rightarrow$

$$\begin{aligned} \kappa(s) &= 4\zeta s \\ \chi(s) &= 2\zeta s^2 \\ x(s) &= \int_0^s \sin(2\zeta u^2)du \\ y(s) &= \int_0^s \cos(2\zeta u^2)du \end{aligned} \quad -\frac{1}{2} \leq s \leq \frac{1}{2} \tag{32}$$

For non symmetrical configurations, one intermediate configuration symmetrical to both initial and final configurations must be found. It belongs to a circle. Then two portions of clothoids must be joined.
For a real clothoid, the following relations are used

1. homothetie $\ell = \frac{d}{D(\zeta)}$
2. rotation $\chi(s) \to \chi(s) + \varsigma$
3. translation $x(s) \to x(s) + x_0$ and $y(s) \to y(s) + y_0$

The loci of split configurations joining the start and end configurations with a bi-elementary path is a circle. Therefore, it exists an infinite set of solutions (bi-elementary paths with different lengths and curvatures) joining start and end configurations. In particular, the shortest bounded curvature path satisfying $\kappa \leq \kappa_{max}$ is of interest.

Spiral Cubic. For symmetrical configurations

$$\begin{aligned} D(\zeta) &= 2\int_0^{0.5} \cos\left(\zeta s\left(\tfrac{3}{2} - 2u^2\right)\right)du \\ \ell &= \tfrac{d}{D(\zeta)}\kappa(s) = \tfrac{6\zeta}{\ell^3}\left(\tfrac{\ell^2}{4} - s^2\right) \\ \chi(s) &= \tfrac{6\zeta}{\ell^3}\left(\tfrac{\ell^2}{4} - \tfrac{s^3}{3}\right) \\ x(s) &= \int_0^s \sin(\chi(u))du \\ y(s) &= \int_0^s \cos(\chi(u))du \end{aligned} \tag{33}$$

The locus of intermediate configurations for non symmetrical initial and final configurations are on

1. if $P_i // P_f$, parallel configurations then it is on the line
$$(x - x_i)(y - y_f) = (x - x_f)(y - y_i)$$
2. it not, the loci is a circle whose center is given by
$$P_c = \left(\frac{x_i + x_f + c(y_i + y_f)}{2}, \frac{y_i + y_f + c(x_i + x_f)}{2}\right)$$
where $c = \left(\tan\frac{\chi_i + \chi_f}{2}\right)^{-1}$

3D Cartesian Cubic polynomials

This problem can be solved by interpolating via Cartesian polynomials using the following cubic polynomials [21] versus a normalized time $0 \leq \tau = \frac{t}{T} \leq 1$

$$\begin{aligned} x(\tau) &= \tau^3 x_f - (\tau - 1)^3 x_i + \alpha_x \tau^2(\tau - 1) + \beta_x \tau(\tau - 1)^2 \\ y(\tau) &= \tau^3 y_f - (\tau - 1)^3 y_i + \alpha_y \tau^2(\tau - 1) + \beta_y \tau(\tau - 1)^2 \\ z(\tau) &= \tau^3 z_f - (\tau - 1)^3 z_i + \alpha_z \tau^2(\tau - 1) + \beta_z \tau(\tau - 1)^2 \end{aligned} \tag{34}$$

that automatically satisfy the boundary conditions on x,y,z. This 3D cubic polynomial has 6 unknowns that can be determined directly. However, there is only one parameter left to respect the limitations on the curvature

and torsion chosen as $T = max(T_1, T_2)$ where T_1, T_2 are respectively the arrival time when the curvature and/or the torsion are saturated.
The orientation at each point being related to x',y',z', it is also necessary to impose the additional boundary conditions

$$\begin{aligned} \dot{x}(0) &= V_i \cos\gamma_i \sin\chi_i \\ \dot{y}(0) &= V_i \cos\gamma_i \cos\chi_i \\ \dot{z}(0) &= V_i \sin\gamma_i \end{aligned} \tag{35}$$

and

$$\begin{aligned} \dot{x}(1) &= V_f \cos\gamma_f \sin\chi_f \\ \dot{y}(1) &= V_f \cos\gamma_f \cos\chi_f \\ \dot{z}(1) &= V_f \sin\gamma_f \end{aligned} \tag{36}$$

Resolving for the various parameters, the following equalities are obtained

$$\begin{aligned} \alpha_x &= TV_f \cos\gamma_f \sin\chi_f - 3x_f \\ \alpha_y &= TV_f \cos\gamma_f \cos\chi_f - 3y_f \\ \alpha_z &= TV_f \sin\gamma_f - 3z_f \end{aligned} \tag{37}$$

and

$$\begin{aligned} \beta_x &= TV_i \cos\gamma_i \sin\chi_i + 3x_i \\ \beta_y &= TV_i \cos\gamma_i \cos\chi_i + 3y_i \\ \beta_z &= TV_i \sin\gamma_i + 3z_i \end{aligned} \tag{38}$$

The evolution of the vehicle orientation along the path can then be computed for the flight path angle

$$\gamma = \arcsin\left(\frac{\dot{z}}{V}\right) \tag{39}$$

and the heading angle

$$\chi = \arctan\left(\frac{\dot{x}}{\dot{y}}\right) + k\pi; \quad k = 0, 1 \tag{40}$$

The two possible choices for k account for the fact that the same Cartesian path may be followed moving forward (k=0) or backward (k=1). If the initial orientation is assigned, only one of the choices for k is correct.

This approach can be easily generalizable to a fourth or fifth polynomial. However the main drawback is a complicated formulation of the curvature and the torsion making control of smoothness (twists and cusps) a difficult task. The approach followed in the following subsection aims to propose an easy formulation of these two parameters.

Pythagorean Hodograph

The above presented curves are defined in terms of the Fresnel integrals which are not rational and not exactly expressible as a non uniform rational B-splines (NURBS). As an alternative, the cubic Bezier and Pythagorean curves can be explored. The Pythagorean

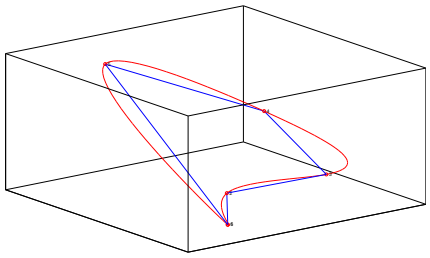

FIGURE 2. Bezier curves

Hodograph (PH) curves are introduced to provide exact solutions to a number of basic computational problems that arise in robot path planning. These include analytic reduction of the arc length and bending energy integrals, construction of rational offset (parallel) curves, formulation of real time interpolator for motion control applications; determination of rotation minimizing frames for specifying orientations of rigid bodies along spatial paths.
The PH condition states that the sum of the squares of the sides of a right-angle triangle is equal to the square of its hypotenuse. In the time domain, the hodograph is called the velocity vector, which is always parallel to the tangent of the path.
The Double Pythagorean Hodograph methodology is used in this paper [10, 14, 25].
For a spatial curve $C(t) = (x(t), y(t), z(t))^T$, the spatial Pythagorean Hodograph (PH) curves are polynomial curves characterized by the fact that their parameter speed $V(t) = |C'(t)|$ is a polynomial in the parameter t. This property is achieved by the a-priori incorporation of a Pythagorean structure in the components of the derivative $C'(t) = (x'(t), y'(t), z'(t))^T$ also called hodograph.
In order to secure a rational dependence of the curvature and the torsion on the curve parameter, it is necessary to incorporate Pythagorean structures into both the first hodograph $C'(t)$ and the cross-product $C'(t) \times C''(t)$ of the first and second hodograph. These curves are called Double Pythagorean Hodograph curves.
A polynomial space curve is said to Double Pythagorean Hodograph (DPH) if the Frenet-Serret frame, the curvature and the torsion have all a rational dependence on the curve parameter.
The simplest non trivial Pythagorean Hodograph are cubic, they correspond to segments of non circular helices with a constant curvature/torsion ratio $\frac{\kappa}{\Gamma}$. They may be characterized by certain geometrical constraints on these Bezier control polygons, see figure 2.

$$r(\tau) = \sum_{k=1}^{3} b_k \binom{3}{k} (1-\tau)^{3-k} \tau^k \qquad \tau \in [0,1] \tag{41}$$

To guarantee sufficient shape flexibility, fifth order Pythagorean Hodograph curve may be employed. The construction of spatial Pythagorean Hodograph fifth order is described, in Bernstein-Bezier form

$$r(\tau) = \sum_{k=1}^{5} b_k \begin{pmatrix} 5 \\ k \end{pmatrix} (1-\tau)^{5-k} \tau^k \qquad \tau = \frac{t}{T} \in [0,1] \tag{42}$$

with

$$\begin{pmatrix} n \\ k \end{pmatrix} = \frac{n!}{k!(n-k)!}$$

where $b_k = (x_k, y_k, z_k)$ are control points, whose vertices define the control polygon or Bezier polygon, t is a parameter and $k = 0...5$.
In 3D, a Pythagorean Hodograph $r(t) = (x(t), y(t), z(t))$ is a polynomial curve whose tangents $\dot{x}(t)$, $\dot{y}(t)$ and $\dot{z}(t)$ satisfies

$$\dot{x}^2(t) + \dot{y}^2(t) + \dot{z}(t) = \sigma^2(t) \tag{43}$$

for some polynomial $\sigma(t)$. From the principles of differential geometry, the path length s and parametric speed $\dot{s}$ of a parametric curve are given by:

$$s = \int_{t_1}^{t_2} \|\dot{r}(t)\| \, dt = \int_{t_1}^{t_2} \sqrt{\dot{x}^2(t) + \dot{y}^2(t) + +\dot{z}^2(t)} dt \tag{44}$$

If the sum of square of the tangents $\dot{x}(t), \dot{y}(t), +\dot{z}(t)$ could be represented by perfect square of a single polynomial, it leads to two advantages:

- The radical form for calculating the path length is eliminated
- The parametric speed of the curve is simply a polynomial function of the parameter t.

The arc length of the Pythagorean Hodograph curve can be computed precisely by evaluating a polynomial. For the hodograph $\dot{r} = (\dot{x}(t), \dot{y}(t), \dot{z}(t))$, it is necessary and sufficient that its components be expressible in terms of polynomials $u(t), v(t), p(t), q(t)$ in the form

$$\begin{aligned} \dot{x}(t) &= u^2(t) + v^2(t) - p^2(t) - q^2(t) \\ \dot{y}(t) &= 2\left(u(t)q(t) + v(t)p(t)\right) \\ \dot{z}(t) &= 2\left(v(t)q(t) - u(t)p(t)\right) \end{aligned} \tag{45}$$

with the corresponding polynomial parameter speed

$$\sigma(t) = u^2(t) + v^2(t) + p^2(t) + q^2(t) \tag{46}$$

If $u(t), v(t), p(t), q(t)$ are all constants, the hodograph is a single point specifying a uniformly parameterized straight line.
For PH fifth orders, $|r' \times r''| = \sigma^2 \iota$ and $\iota = (up' - u'p + vq' - v'q)^2 + (uq' - u'q + v'p - vp')^2$.
For PH fifth order, $(r' \times r'').r'''$ is of degree 6 while σ, ι are both in degree 4 in t.
The minimum order polynomial that exhibits the PH behavior is the third and is called the cubic PH. However the lowest order of the PH path that has a point of inflection is the fifth, called the quintic PH. The presence of an inflection point allows the path to have more flexibility so that the path can be easily manipulated. Hence, the quintic PH curve is used for path planning for autonomous aircrafts.
if the polynomials $u(t), v(t), p(t), q(t)$ are of degree m at most, the PH curve $C(t)$ obtained by integrating the hodograph $C'(t)$ is of odd degree $(2m+1)$ For a PH curve with $\iota = \omega^2$, the Frenet frame vectors and the curvature and torsion functions are given by the rational expressions:

$$T = \frac{r'}{\sigma} = \frac{1}{V} \begin{pmatrix} u^2 + v^2 - p^2 - q^2 \\ 2(uq + vp) \\ 2(uq + vp) \end{pmatrix} \tag{47}$$

and

$$\begin{aligned} N &= \frac{\sigma r'' - \sigma' r'}{\sigma \omega} \\ B &= \frac{r' \times r''}{\sigma \omega} \\ \kappa &= \frac{\omega}{\sigma^2} \\ \Gamma &= \frac{(r' \times r'').r'''}{\sigma^2 \omega^2} \end{aligned} \tag{48}$$

Hence, the PH curves may be regarded as the complete set of polynomial curves that have rational Frenet frame. Let the initial and final configurations be $(x_i, y_i, z_i, \chi_i, \gamma_i, V_i)^T$ and $\left(x_f, y_f, z_f, \chi_f, \gamma_f, V_f\right)^T$. The four control points of the Bezier polygon are calculated by first order Hermite interpolation as follows:

$$\begin{aligned} b_0 &= (x_i, y_i, z_i) \\ b_5 &= \left(x_f, y_f, z_f\right) \\ b_1 &= b_0 + TV_i \tfrac{1}{5} \left(\sin\chi_i \cos\gamma_i, \cos\chi_i \cos\gamma_i, \sin\gamma_i, \right) \\ b_4 &= b_5 - TV_f \tfrac{1}{5} \left(\sin\chi_f \cos\gamma_f, \cos\chi_f \cos\gamma_f, \sin\gamma_f, \right) \end{aligned} \tag{49}$$

The control points b_0, b_1, b_4, b_5 are fixed. Now the problem is reduced to finding the control points b_2, b_3. Both polynomials curves are given by

$$\begin{aligned} u(t) &= u_0(1-\tau)^2 + 2u_1(1-\tau)\tau + u_2\tau^2 \\ v(t) &= v_0(1-\tau)^2 + 2v_1(1-\tau)\tau + v_2\tau^2 \\ p(t) &= p_0(1-\tau)^2 + 2p_1(1-\tau)\tau + p_2\tau^2 \\ q(t) &= q_0(1-\tau)^2 + 2q_1(1-\tau)\tau + q_2\tau^2 \end{aligned} \tag{50}$$

Knowing that

$$\int \begin{pmatrix} n \\ k \end{pmatrix} (1-t)^{n-k} t^k dt = \frac{1}{n+1} \sum_{i=k+1}^{n+1} (1-t)^{n+1-i} t^i \tag{51}$$

The set of equations to be solved for the control points b_2, b_3 results in four solutions. Among these four paths, only one has an acceptable shape that is without twists and cusps. This path will be used as reference and is identified by calculating the bending energy of the curve and choosing the path whose energy is minimal.

CONCLUSIONS

The problem of characterizing continuous paths in 3D is addressed with constraints on curvature and torsion, as consequence from limitations on thrust and velocity. Parametric paths are investigated, depending on the initial and final configurations. Smoother paths can be obtained by asking for the continuity of the derivatives of the path curvature and torsion. This paper addresses the problem of characterizing continuous paths in 3D.
The role of the trajectory generator is to generate a feasible time trajectory for the autonomous aircraft. Once the path has been calculated in the Earth fixed frame, motion must be investigated and reference trajectories determined taking into account actuators constraints.
Trajectory planning incorporates dynamics into planning processes. Depending on the mission, time variable velocity must be considered, giving more flexibility to the trajectory generator, with respect to the limitations on actuators, on curvature and torsion.Parametric paths with given curvature and torsion are investigated. It is important for the autonomous aircraft to follow paths that are not discontinuous in curvature. Maneuvers should be kept only to join two trim flight paths. Finally, some parametric curves such as Double Pytaghorean Hodograph with Bernstein-Bezier polynomials, are presented.

REFERENCES

1. Ambrosino, G., Ariola, M., Ciniglio, U., Carraro, F., Delellis, E., Pironti, A. : *Path Generation and Tracking in 3D for UAVs*, IEEE Trans. on Control System Technology, **17**, 980–988 (2009)
2. Avanzini, G. : *Frenet based algorithm for trajectory prediction*, AIAA J. of Guidance, control and dynamics, **27**, 127–135 (2004).
3. Babaei, A. R., Mortazavi, M. : *Three dimension curvature constrained trajectory planning based on in-flight waypoints* AIAA J. of Aircraft, **47**, 1391–1398 (2010).
4. Bestaoui, Y. : *Geometric Properties of Aircraft Equilibrium and Non Equilibrium Trajectory Arcs*. K. Kozlowski ed., Springer, Lectures Notes in Control and Information Sciences, (2009)
5. Bestaoui, Y. : *Mission plan under uncertainty for an autonomous aircraft* Proc. of the Institution of Mechanical Engineers, part G: J. Of Aerospace Engineering, **24**, 1297–1307 (2010)
6. Bestaoui, Y. : *Lighter Than Air Robots*, Springer, 2012.
7. de Boor, C : *A practical guide to splines*, Springer, (2001)
8. Choi, H.I, Lee, D. S., Moon, H. P. : *Clifford algebra, spin representation and rational parameterization of curves and surfaces*, Advanced Computer Mathematics, **17**, 5–48, (2002)
9. De Filippis, L., Guglieri, G. *Path planning strategies for UAV in 3D environments* Journal of Intelligent and Robotics Systems, vol. 65, pp. 247-264 (2012)
10. Farouki : *Pythagorean Hodograph Curves*, Springer (2008).
11. Farouki, R. T. , Giannelli, C. , Sestini A. : *Helical polynomial curves and Double Pythagorean Hodographs I-Quaternion and Hopf map representations*, J. of Symbolic Computation, **44**, 161–179 (2009).
12. Farouki, R. T. , Giannelli, C. , Sestini A. : *Helical polynomial curves and Double Pythagorean Hodographs II-Enumeration of low degree curves*, J. of Symbolic Computation, **44**, 307–332 (2009).
13. Fraichard, T, Scheuer, A. : *From Reeds and Shepp's to Continuous Curvature Paths*. IEEE Trans. on Robotics. **20**, 1025–10355 (2008)
14. Jaklic, G. , Kozak,J., Krajnc, M.,Vitrih, V. , Zagar E. : *Geometric Lagrange Interpolation by planar cubic Pythagorean Hodograph curves*, Computer Aided Design (2008)
15. Kanayama, Y., Miyake, N. : *Trajectory Generation for Mobile Robots*. Robotics Research. **3**, 333–340 (1986)
16. Lafferiere, G., Sussmann,J. H. : *A Differential Geometric Approach to Motion Planning*, Kluwer 1993.
17. McGee, T. , Hedrick, J.K. : *Optimal path planning with a kinematic airplane model*. AIAA J. of Guidance, Control and Dynamics, **30**, (2007)
18. Nelson, R., Barber, B., McLain, T., Beard, R.: *Vector Field Path Following for Miniature Air Vehicle*. IEEE Trans. on Robotics. **23**, 519–529, (2007)
19. Piazzi, A., Guarino Lo Bianco, C., Romano, M. : η^3 *Splines for the smooth path generation of wheeled mobile robot* , IEEE Trans. on Robotics, **5**, 1089–1095 (2007)
20. Serakos, D., Lin, C. F. : *Three dimensional mid-course guidance state equations*. American Control Conf., 3738–3742 (1999)
21. Siciliano, B., Sciavicco, L., Villani, L., Oriolo, G. : *Robotics, modelling, planning, and control*. Springer (2009)
22. Shanmugavel, M. ,Tsourdos, A. , Zbikowski, R. , White, B. A., Rabbath, C. A., Lechevin, N. : *A solution to simultaneous arrival of multiple UAV using Pythagorean hodograph curves* American Control Conference, Minneapolis, MN, 2813–2818 (2006)
23. Soueres, P., Laumond, J.P. : *Shortest Paths Synthesis for a Car-like Robot*. IEEE Trans. on Robotics. **41**, 672–688 (1996)
24. Tsourdos, A. , White, B. A., Shanmugavel, M. : *Cooperative path planning of unmanned aerial vehicles* Wiley (2010)
25. Walton, D. J., Meek, D. S. :*Planar G^2 curve design with spiral segments*, Computer Aided Design, **30**, 529–538, (1998)